Compartmentalization of visual centers in the *Drosophila* brain requires Slit and Robo proteins

Timothy D. Tayler, Myles B. Robichaux* and Paul A. Garrity†

Department of Biology, Massachusetts Institute of Technology, 77 Massachusetts Avenue 68-230B, Cambridge, MA 02139, USA
*Present address: Louisiana State University Health Sciences Center, New Orleans, LA 70112, USA
†Author for correspondence (e-mail: pgarrity@mit.edu)

Accepted 23 September 2004

Development 131, 5935-5945
Published by The Company of Biologists 2004
doi:10.1242/dev.01465

Summary

Brain morphogenesis depends on the maintenance of boundaries between populations of non-intermingling cells. We used molecular markers to characterize a boundary within the optic lobe of the *Drosophila* brain and found that Slit and the Robo family of receptors, well-known regulators of axon guidance and neuronal migration, inhibit the mixing of adjacent cell populations in the developing optic lobe. Our data suggest that Slit is needed in the lamina to prevent inappropriate invasion of Robo-expressing neurons from the lobula cortex. We show that Slit protein surrounds lamina glia, while the distal cell neurons in the lobula cortex express all three *Drosophila* Robos. We examine the function of these proteins in the visual system by isolating a novel allele of *slit* that preferentially disrupts visual system expression of Slit and by creating transgenic RNA interference flies to inhibit the function of each *Drosophila* Robo in a tissue-specific fashion. We find that loss of Slit or simultaneous knockdown of Robo, Robo2 and Robo3 causes distal cell neurons to invade the lamina, resulting in cell mixing across the lamina/lobula cortex boundary. This boundary disruption appears to lead to alterations in patterns of axon navigation in the visual system. We propose that Slit and Robo-family proteins act to maintain the distinct cellular composition of the lamina and the lobula cortex.

Key words: Glia, Neuron, Compartment boundary, Optic lobe, *Drosophila*

Introduction

The establishment of compartments, groups of adjacent but non-intermingling cells, is a common method for creating organization during development, and the mechanisms underlying the generation of cellular compartments has been extensively studied (Dahmann and Basler, 1999; Irvine and Rauskolb, 2001; McNeill, 2000; Vegh and Basler, 2003). Compartmentalization plays a crucial role in the development of the nervous system, and multiple compartments have been defined in the developing vertebrate forebrain, midbrain and hindbrain (Irvine and Rauskolb, 2001; Larsen et al., 2001; Lumsden and Krumlauf, 1996; Redies and Puelles, 2001; Zeltser et al., 2001). Transcription factors, such as Kreisler (Mafb – Mouse Genome Informatics) (Cordes and Barsh, 1994) and Krox-20 (Egr2 – Mouse Genome Informatics) (Schneider-Maunoury et al., 1997), and cell-cell signaling proteins, such as Notch and regulators of Notch signaling (Cheng et al., 2004; Zeltser et al., 2001), have been identified that have crucial roles in establishing compartment boundaries during nervous system development. These proteins have been proposed to affect cell mixing between compartments by regulating the expression or activity of factors that confer distinct affinities upon cells of different compartments (Dahmann and Basler, 1999; Irvine and Rauskolb, 2001; McNeill, 2000; Vegh and Basler, 2003).

Mechanisms that have been proposed to restrain cell mixing between compartments include preferential adhesion among cells within a compartment, preferential adhesion between cells of different compartments at the compartment boundary, and mutual repulsion between cells of different compartments (Dahmann and Basler, 1999; Irvine and Rauskolb, 2001; McNeill, 2000; Milan et al., 2001). Members of the Cadherin family of adhesion molecules and the Eph/Ephrin family of repellant signaling proteins have been implicated in regulating cell mixing between compartments in the developing vertebrate nervous system (Cooke and Moens, 2002; Inoue et al., 2001; Redies, 2000; Xu et al., 2000). In-vitro reconstitution experiments have shown that differential Cadherin expression or Eph/Ephrin signaling is sufficient to create groups of non-intermingling cells (Mellitzer et al., 1999; Nose et al., 1988), while ectopic expression and dominant-negative studies have shown that these proteins can alter cell sorting in vivo (Cooke and Moens, 2002; Inoue et al., 2001; Xu et al., 1999). However, loss-of-function analysis has not yet demonstrated a requirement for either Cadherin expression or Eph/Ephrin signaling in restricting cell movement between compartments of the developing brain (Cooke and Moens, 2002; Inoue et al., 2001).

The developing *Drosophila melanogaster* brain, like the vertebrate brain, contains many compartments that give rise to multiple, anatomically distinct processing centers, and recent work has begun to detail the morphogenetic events of fly brain development comprehensively (Dumstrei et al., 2003; Hartenstein et al., 1998; Meinertzhagen et al., 1998; Nassif et al., 2003; Younossi-Hartenstein et al., 2003). The visual centers

of the fly brain, the optic lobes, contain four ganglia (the lamina, medulla, lobula and lobula plate), which are derived from two distinct populations of progenitor cells, the outer and inner optic anlagen (Hofbauer and Campos-Ortega, 1990; Meinertzhagen and Hanson, 1993; Younossi-Hartenstein et al., 1996). Progeny of the outer optic anlagen contribute to the lamina and outer medulla, while progeny of the inner optic anlagen contribute to the inner medulla, lobula and lobula plate. Descendents of these different anlagen lie adjacent to one another during development without intermingling and act as distinct developmental compartments within the brain. For example, the neurons and glia of the developing lamina, derived from the outer optic anlagen (Dearborn and Kunes, 2004; Meinertzhagen and Hanson, 1993), lie immediately adjacent to the neurons of the developing lobula cortex, which are derived from the inner optic anlagen (Hofbauer and Campos-Ortega, 1990; Meinertzhagen and Hanson, 1993), but the two cell populations remain distinct. How these cell populations are prevented from intermingling is unknown.

The Slit and Robo protein families are essential for axon guidance and cell migration in worms, flies, fish and mice (Brose and Tessier-Lavigne, 2000; Wong et al., 2002). Slits are secreted proteins that can act as either attractive or repulsive guidance cues (Englund et al., 2002; Kramer et al., 2001), while members of the Robo family encode transmembrane receptors for Slits (Brose et al., 1999; Rajagopalan et al., 2000b; Simpson et al., 2000b). *Drosophila* has a single Slit receptor and three Robo receptors [Robo, Robo2 (Leak – FlyBase) and Robo3] (Kidd et al., 1999; Rajagopalan et al., 2000a; Rajagopalan et al., 2000b; Simpson et al., 2000a; Simpson et al., 2000b). The recent identification of mutations in human ROBO3 (RIG1) in individuals with horizontal gaze palsy and progressive scoliosis with hindbrain dysplasia demonstrates that ROBO-receptor function is also important for human brain development (Jen et al., 2004).

In the present work, we identify members of the Slit and Robo families as key factors that limit cell mixing between two adjacent cell populations in the *Drosophila* brain, the lamina glia and the distal cell neurons of the lobula cortex. We characterize a set of molecular markers that permit us to examine the behavior of cells at the boundary between the lamina and the lobula cortex. We find that Slit protein surrounds the lamina glia, while the distal cell neurons of the lobula cortex express multiple Robo family receptors. We show that either loss of Slit or the tissue-specific knockdown of multiple Robo family members causes distal cell neurons to intermingle with the lamina glia, disrupting the boundary between the lamina and lobula cortex. We propose that Slit and Robo family proteins prevent cell mixing at the lamina/lobula interface, enforcing a boundary between adjacent compartments of the developing *Drosophila* brain that is essential for morphogenesis of the visual system.

Materials and methods

Genetics and fly stocks

The $slit^{dui}$ phenotype was originally identified in *l(2)k04807* (Karpen and Spradling, 1992; Torok et al., 1993). *l(2)k04807* contains pLacW P-element transposon insertions located at 52D and 53C, which were separated by meiotic recombination. $slit^{dui}$ was associated with the 52D P-element, which was inserted between bases 10,983,983 and 10,983,984 on 2R with the *lacZ* coding region oriented toward the *slit* locus. (Slit transcript extends from bases 10,954,579 to 10,936,369.) Precise transposon excision reverted $slit^{dui}$ phenotype in all 11 lines tested. $slit^{l(2)k05248}$ (Karpen and Spradling, 1992; Torok et al., 1993) contains a pLacW transposon inserted between bases 10,985,837 and 10,985,838 on 2R, with the *lacZ* coding region oriented away from the *slit* locus. Mosaic analysis with a repressible cell marker (MARCM) was performed as described (Lee and Luo, 1999). Fly stocks $slit^{2}$, $slit^{l(2)k05248}$, *Df(2R)WMG*, *Df(2R)Jp1*, Omb-Gal4, repo-*lacZ*, and *c155-Gal4* were obtained from the Bloomington Stock Center. $slit^{E158}$, $slit^{2}$; *UAS-Slit*, $loco^{3–109}$, $robo^{5}$ and robo2^{x123} were provided by J. Simpson, G. Bashaw and C. Goodman; $robo3^{1}$ (Rajagopalan et. al., 2000b) by B. Dickson; *Ro-τ-lacZ* by U. Gaul; and eya^{2} by I. Rebay.

Immunohistochemistry and in-situ hybridization

Third-instar whole mounts were performed as described (Garrity et al., 1996). Distal cell neuron positioning, glial positioning and photoreceptor axon targeting defects were observed in all *slit* and triple Robo family RNA interference (RNAi) animals examined and more than 20 hemispheres were examined for each genotype. The following primary antibodies were obtained from the Developmental Studies Hybridoma Bank and used at the concentrations indicated: 24B10 mAb (1:200); Slit C555.6D (1:200); Robo mAb 13C9 (1:200); Robo3 mAb 14C9 (1:200); Fas2 1D4 (1:200); Fas3 7G10 (1:50); Repo 8D12 (1:200); Elav 7E8A10 (1:20); and β-galactosidase 40-1A (1:200). Robo2 polyclonal antisera (1:750) (Rajagopalan et al., 2000b; Simpson et al., 2000a) were provided by C. Goodman and by B. Dickson, and Repo polyclonal (1:1000) (Campbell et al., 1994) by A. Tomlinson. Anti-phosphohistone H3 (1:200) was purchased from Upstate Biotechnology. Secondary antibodies were obtained from Jackson Laboratories and used at the following concentrations: goat-anti-mouse hrp-conjugated (1:200); goat-anti-mouse Cy3-conjugated (1:500); goat-rat-mouse Cy5-conjugated (1:400). Fluorescent samples were visualized using a Nikon PCM2000 confocal microscope. In-situ hybridization was performed as described (Wolff, 2000).

Molecular biology

Genomic DNA flanking the $slit^{dui}$ P-element was isolated by plasmid rescue and sequenced to identify the insertion site as described (Garrity et al., 1996). Western blot analysis used the following antibodies: Robo mAb 13C9 (1:2000); Robo3 mAb 14C9 (1:1000); Elav 7E8A10 (1:1000); anti-hrp-conjugated secondary antibody (1:5000). Robo family RNAi constructs were generated using the strategy described (Kalidas and Smith, 2002). Fragments for creating the RNAi constructs were generated by PCR (Expand Hi-Fidelity, Roche) and cloned into pUASt (Brand and Perrimon, 1993). PCR primers used to create UAS-RoboRNAi were: genomic fragment 5′-ACCGGGCAGCTGATCCTAGC and 5′-ATACTAGTCTGTC-GAATAATAAGAAGATATAAAATGATTC; cDNA fragment 5′-TGTCAGTCGCACCAGCATTAGTC and 5′-ATACTAGTCATC-TTCATAGGTGAGGGCTGTC. PCR primers used to create UAS-Robo2RNAi were: genomic fragment 5′-GTTCCCTCTGAGGCAC-CATATG and 5′-ATACTAGTGTGTGATTGCCTGCAGGTGAG; cDNA fragment 5′-GTTCCCTCTGAGGCACCATATG and 5′-AT-ACTAGTCCACGCATTGTATTTAGGGCCG. PCR primers used to create UAS-Robo3RNAi were: genomic fragment 5′-TATA-TCGCAGTGGCGGCTGCC and 5′-ATAGATCTCTGCAATTG-GAGGGGATGAAATCAG; cDNA fragment 5′-TATATCGCAGT-GGCGGCTGCC and 5′-ATAGATCTCTCTCGTAATCGGGTAG-CAGC.

Results

Organization of the developing optic lobe

The optic lobes are comprised of four processing centers

derived from two distinct populations of precursor cells. In several regions of the optic lobe, cells derived from these different sets of progenitors lie immediately adjacent to one another but do not intermingle. This type of organization is found at the interface of the lamina and the lobula cortex, which are derived from the outer and inner optic anlagen, respectively. As shown in the horizontal section in Fig. 1A and represented in Fig. 1C, distal cell neurons form the anterior edge of the lobula cortex and are located immediately adjacent to the posterior face of the lamina (dotted yellow line denotes anterior edge of lobula cortex, Fig. 1A). The close apposition of distal cell neurons to the glia at the posterior edge of the developing lamina is visible in the lateral section in Fig. 1B and represented in Fig. 1D. In the present work, we examine the mechanisms that prevent the distal cell neurons of the lobula cortex from intermingling with the lamina glia.

Slit is required for optic lobe morphogenesis

Our examination of the lamina/lobula cortex boundary initiated with the identification from a genetic screen of a novel allele of *slit*, $slit^{dui}$ *(dui, disrupted innervation)*, which severely disrupted photoreceptor axon innervation of the optic lobe (Fig. 2A-D). We found that $slit^{dui}$ was caused by insertion of a transposable element 29,404 bases upstream of the 5′ end of the Slit transcript (see Materials and methods for details). Similar photoreceptor connectivity defects were obtained when $slit^{dui}$ was examined in combination with other *slit* loss-of-function alleles, including the transposon insertion alleles $slit^{l(2)k05248}$ (described in greater detail below) and $slit^{E158}$ (Battye et al., 2001) (Fig. 2E,F). In particular, the photoreceptor connectivity phenotypes of $slit^{dui}/slit^{2}$ animals ($slit^{2}$ is a previously characterized null) (Kidd et al., 1999) were indistinguishable from those of $slit^{dui}/slit^{dui}$ animals indicating that $slit^{dui}$ behaved as a recessive strong loss-of-function allele in the visual system (Fig. 2G). However, unlike previously described strong alleles of *slit*, which die before the development of the adult optic lobe, $slit^{dui}$ mutants were homozygous viable, greatly facilitating analysis of *slit* function in the visual system. As shown below, $slit^{dui}$ significantly reduced Slit expression in the optic lobes without completely eliminating Slit expression in other regions. The *slit* photoreceptor connectivity defect could be rescued by expression of a Slit cDNA in the visual system under the control of Omb-Gal4 (Fig. 2H), which drives expression broadly in optic lobe glia and in a subset of optic lobe neurons (Dearborn and Kunes, 2004; Rangarajan et al., 1999) and restores expression of Slit in the optic lobe neuropils (data not shown). Examination of the photoreceptor axon target region in *slit* mutants showed that the lamina glia, intermediate targets of R1-R6 photoreceptor axons, were also disrupted (Fig. 2I,J), and that regions of photoreceptor axon mistargeting correlated with areas of lamina glial disruption (Fig. 2K,L). This raised the possibility that the photoreceptor axon targeting defects in *slit* mutants could be a secondary consequence of other disruptions in optic lobe development.

Slit prevents distal cell neurons from entering the lamina

The disrupted positioning of lamina glia in *slit* mutants prompted us to examine whether the adjacent distal cell neurons might be disorganized as well. In Fig. 3, postmitotic neurons were visualized with the nuclear marker Elav (blue), while the distal cell neurons and their neuroblast progenitors in the inner proliferation

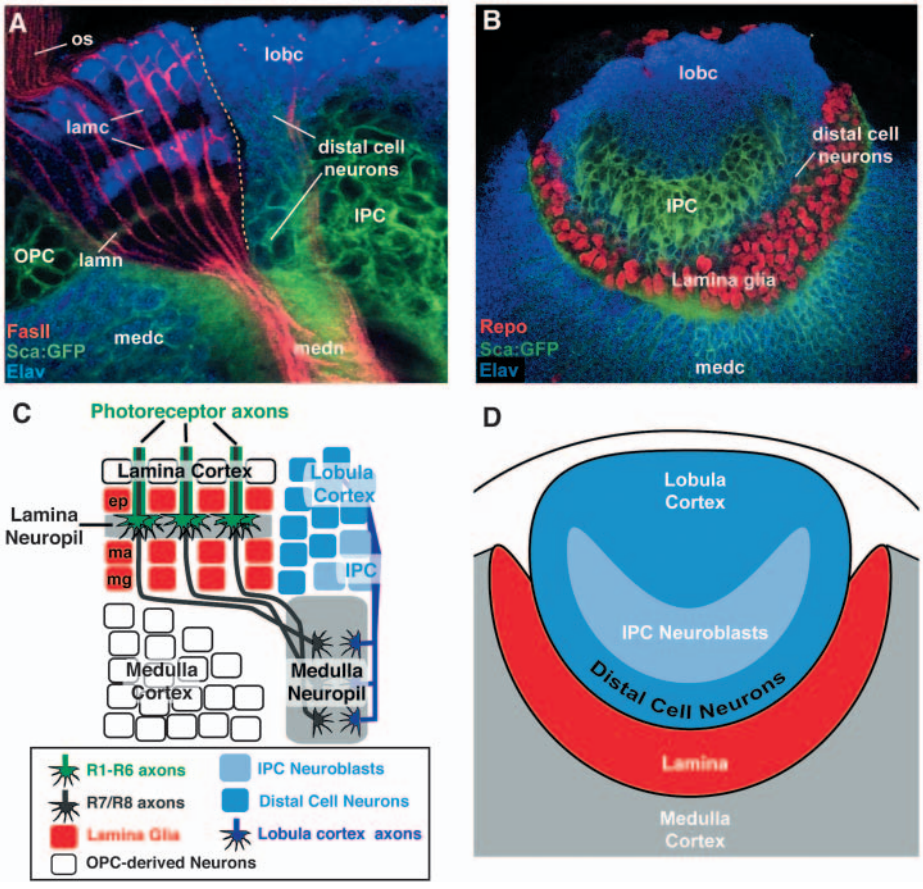

Fig. 1. Developing *Drosophila* visual system. (A) Horizontal view of wild-type third instar visual system (anterior to left) of animal expressing CD8:GFP under the control of *Sca-Gal4* (Sca:GFP). GFP is expressed in the OPC, IPC, medulla cortex and portions of the lobula cortex. Sca:GFP (green). Neuronal nuclei are visualized using anti-Elav (blue); photoreceptor axons, lamina monopolar axons and axons from neurons of the lobula cortex (a subset of which contact the medulla neuropil) are visualized using anti-Fasciclin 2 (Fas2) (red). Dotted line indicates anterior edge of lobula cortex. (B) Lateral view (anterior at bottom) of Sca:GFP animal in which neuronal nuclei have been visualized using anti-Elav (blue) and glial nuclei using anti-Repo (red). Schematics of (C) horizontal view and (D) lateral view, indicating cell populations and axons described in the text. ep, epithelial glia; IPC, inner proliferation center; lamc, lamina cortex; lamn, lamina neuropil; lobc, lobula cortex; ma, marginal glia; medc, medulla cortex; mg, medulla glia; medn, medulla neuropil; OPC, outer proliferation center; os, optic stalk.

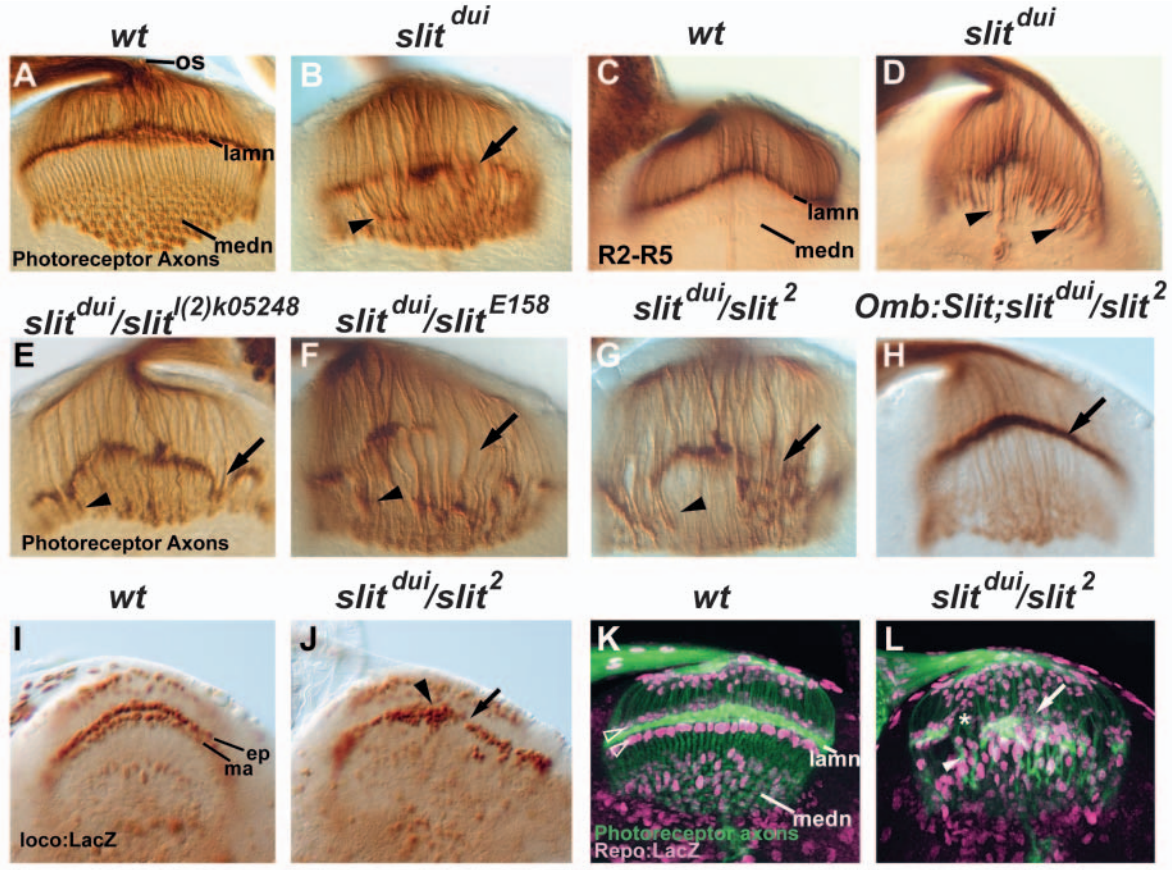

Fig. 2. *Slit* is required for optic lobe development. (A,B,E-H) Third instar visual systems, photoreceptor axons visualized with anti-Chaoptin. (A) In wild type, photoreceptor axons grow into the brain through the optic stalk. The R1-R6 subset of photoreceptor axons stop in the lamina neuropil while R7 and R8 continue into the medulla neuropil. (B) In $slit^{dui}$ mutants, there are gaps in the lamina neuropil (arrow) and increased numbers of axons enter the medulla (arrowhead). (C) Wild type and (D) $slit^{dui}$ visual systems in which R2-R5 photoreceptor axons are visualized using Ro-τ-*lacZ* (Garrity et al., 1999). (C) In wild type, all R2-R5 axons stop in the lamina neuropil. (D) In $slit^{dui}$ mutants, many R2-R5 axons pass through the lamina and enter the medulla (arrowheads). (E) $slit^{dui}/slit^{l(2)k05248}$, (F) $slit^{dui}/slit^{E158}$ and (G) $slit^{dui}/slit^{2}$ animals show photoreceptor axon targeting defects indistinguishable from $slit^{dui}$ homozygotes, with gaps in the lamina (arrow) and increased numbers of axons entering the medulla (arrowhead). (H) *Omb-Gal4;UAS-Slit;* $slit^{dui}/slit^{2}$ visual system. Slit cDNA expression controlled by *Omb-Gal4* largely rescues *slit* targeting defects, restoring even layer of photoreceptor growth cones in the lamina (arrow). (I,J) Animals carrying *loco:lacZ* enhancer trap (which is strongly expressed in epithelial and marginal glia) stained with anti-*lacZ*. (I) In wild type, continuous layers of epithelial and marginal glia are observed in the lamina. (J) In *slit* mutants, there are clumps of glia (arrowhead) and gaps (arrow) in the glial layers. (K,L) Photoreceptors axons are visualized with GMR:GFP (green) and glial nuclei with Repo:*lacZ* (magenta). (K) In wild type, R1-R6 axons stop in the lamina between layers of glia (open arrowheads). (L) In *slit* mutants, there are gaps in the photoreceptor innervation of the lamina, correlated with regions of the lamina devoid of glia (asterisk) and uneven innervation in regions containing clumps of glia (arrow). The clear separation between glia at the base of the lamina and glia surrounding the medulla observed in wild type is missing in *slit* mutants (arrowhead). ep, epithelial glia; lamn, lamina neuropil; ma, marginal glia; medn, medulla neuropil.

center (IPC) were visualized using the cell-surface marker Fasciclin 3 (red), and the lamina was visualized using the photoreceptor axon marker GMR:GFP (green). In wild type, the distal cell neurons never entered the lamina (Fig. 3A). However, in *slit* mutants, many distal cell neurons entered the base of the lamina (arrow, Fig. 3B) and some distal cell neurons invaded the lamina neuropil, disrupting photoreceptor innervation (asterisk, Fig. 3B). A lateral cross-section near the base of the lamina further demonstrated that the normally precise boundary between distal cell neurons and the lamina neuropil (Fig. 3C) was disrupted in *slit* mutants, with large numbers of distal cell neurons invading the lamina neuropil (arrow and arrowhead in Fig. 3D). These data demonstrate that in the absence of *slit*, distal cell neurons invaded the developing lamina.

Slit protein concentrates in the lamina

To further investigate Slit function in visual system development, the pattern of Slit expression was examined in third instar larvae. In the visual system, Slit protein expression was detected in the medulla neuropil and at the base of the lamina (arrow) (Fig. 4A). Consistent with genetic evidence that $slit^{dui}$ is a strong loss-of-function allele in the visual system, Slit expression in the optic lobe was greatly reduced in $slit^{dui}$ mutants (Fig. 4B). Slit was also expressed within the midline of the ventral ganglion and in the mushroom bodies. Slit expression was partially reduced in the ventral ganglion in $slit^{dui}$ mutants, but not visibly altered in the mushroom bodies (Fig. 4B). Such residual Slit expression may explain why $slit^{dui}$ mutants were viable and did not show the midline axon

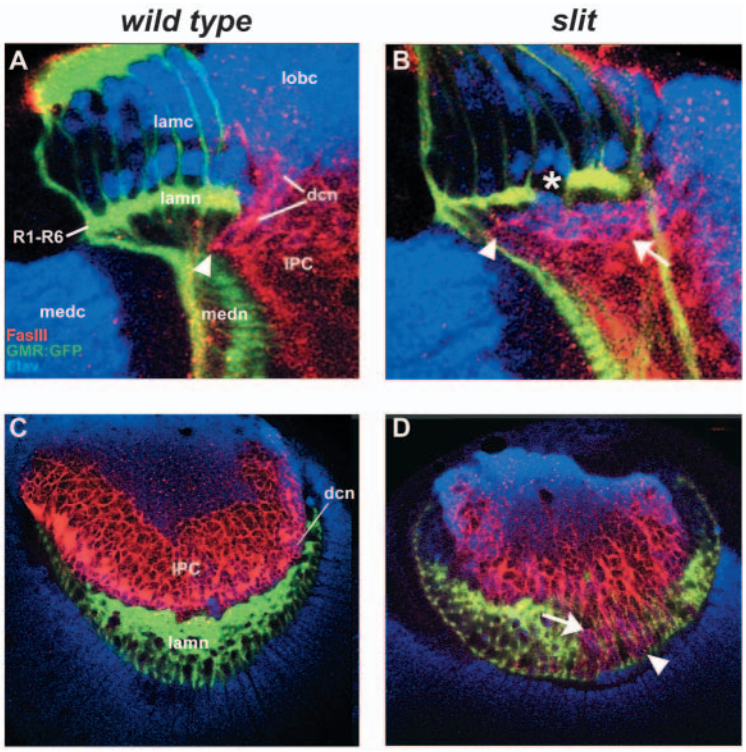

Fig. 3. Distal cell neurons invade the lamina in *slit* mutants. (A-D) Third instar visual systems in which IPC neuroblasts and distal cell neurons are visualized using anti-Fasciclin 3 (Fas3, red), photoreceptor axons using GMR:GFP (green), and neuronal nuclei using anti-Elav (blue). (A,B) Horizontal view (anterior to left). (A) In wild type, IPC neuroblasts (which express Fas3) and their distal cell neuron progeny (which express Fas3 and Elav) are adjacent to the posterior edge of the lamina (arrowhead). (B) In $slit^{dui}/slit^{2}$ mutants, distal cell neurons enter the base of the lamina (arrow) and reach the lamina's anterior edge (arrowhead). Distal cell neurons also enter the neuropil of the lamina (asterisk) and photoreceptor innervation is disrupted. (C,D) Lateral view (anterior at bottom). (C) In wild type, distal cell neurons are immediately adjacent to the posterior face of the lamina. (D) In $slit^{dui}/slit^{2}$ mutants, distal cell neurons enter the posterior face of the lamina (arrow) and reach its anterior edge (arrowhead). dcn, distal cell neuron progeny; IPC, inner proliferation center; lamc, lamina cortex; lamn, lamina neuropil; lobc, lobula cortex; medc, medulla cortex; medn, medulla neuropil.

guidance defects observed in lethal alleles of *slit* (T.D.T. and P.A.G., unpublished data). Taken together, these data demonstrated that Slit was expressed in the optic lobe and that $slit^{dui}$ reduced optic lobe expression of Slit.

The expression of Slit was examined in greater detail. Slit mRNA production was detected within the optic lobes, with strongest expression near the medulla neuropil (Fig. 4C). Simultaneous staining for the glial-specific nuclear protein Repo (green) and Slit protein (magenta) demonstrated that Slit was concentrated throughout the medulla neuropil within the region demarcated by the medulla neuropil glia (Fig. 4D). Slit protein was also present near the base of the lamina. Three layers of glial cells, epithelial glia, marginal glia, and medulla glia, reside in this region, and Slit protein concentrated around them (Fig. 4E). When Slit protein was observed in the absence of Repo staining, Slit localization around these glia gave the base of the lamina a honeycomb appearance (Fig. 4F). A horizontal section demonstrated that Slit was present immediately adjacent to the distal cell neurons (Fig. 4G). Thus, Slit protein was found in a relatively continuous fashion from the lamina neuropil into the medulla neuropil (represented in Fig. 4H). The region of Slit protein concentration was immediately adjacent to the distal cell neurons, demonstrating that Slit protein was present at the appropriate time and place to control the behavior of distal cell neurons.

As the ingrowth of photoreceptor axons induces many developmental events in the optic lobe, we tested whether Slit production depended upon photoreceptor axon innervation. Slit protein was still present in the optic lobe of *eyes absent* (*eya*) mutant animals that had no photoreceptor neurons, indicating that photoreceptor axon innervation was not essential for Slit production (Fig. 4I).

To begin to further characterize the identity of the cells producing Slit protein in the optic lobe, we examined optic lobe expression of an enhancer trap transposon insertion in the Slit locus. The $slit^{l(2)k05248}$ insertion is located 30,258 bases upstream of the Slit mRNA start site, 1853 bases from the $slit^{dui}$ insertion site, and behaves as a loss-of-function *slit* allele in the visual system (see Fig. 2E). Expression of the *lacZ* enhancer trap in $slit^{l(2)k05248}$ resembled the Slit RNA in-situ pattern, with strong expression in the optic lobe and in the midline of the ventral ganglion, and is referred to here as Slit:*lacZ*. Slit:*lacZ* was expressed at the base of the lamina by the medulla glia, the most basal of the three layers of lamina glia (Fig. 4J). Slit:*lacZ* was also expressed by cells in the medulla cortex (Fig. 4J). These cells lay immediately adjacent to the glia that surround the medulla neuropil (Fig. 4K) and appear to be differentiating neurons of the medulla cortex as they express varying levels of the neuronal marker Elav (Fig. 4L). Medulla cortex neurons are known to project axons into the medulla neuropil and could thus deliver Slit protein to the medulla neuropil region. These Slit:*lacZ* enhancer trap data combine with the Slit protein and RNA in-situ data to provide a consistent picture, in which expression of Slit, a diffusible protein, by cells at the base of the lamina and at the periphery of the medulla generate a region of Slit expression extending from the lamina into the medulla.

Distal cell neurons express Robo family proteins

Robo family receptors commonly mediate responses to Slit proteins, so we characterized the distribution of the three *Drosophila* Robo proteins in the developing visual system. Robo, Robo2 and Robo3 were all expressed within the developing optic lobes (Fig. 5A,D,G). More detailed analysis of Robo and Robo2 expression showed that both proteins were expressed by IPC neuroblasts and distal cell neurons (Fig. 5B,C,E,F). Robo3 protein was not detected on IPC neuroblasts, but was present on distal cell neurons (Fig. 5H,I). Thus, all three Robo receptors were expressed within the developing lobula cortex in partially overlapping patterns, consistent with Robo family receptors mediating responses to Slit in this region of the visual system.

Inhibition of Robo family protein expression using transgenic RNAi

The expression patterns of Robo proteins suggested they could

mediate the effects of Slit on distal cell neurons. To begin to address this question, we examined existing loss-of-function mutations in *robo*, *robo2* and *robo3*. Animals homozygous for the previously described strong loss-of-function alleles *robo2*^{x123} or *robo3*^{1} had no detectable defect in distal cell neuron positioning. Distal cell neuron positioning could not be examined in animals homozygous for null alleles of *robo*, because they died before the third instar larval stage. Large marked clones homozygous mutant for the *robo*^{5} null allele were generated in the visual system, but no defects were detected.

As *robo*, *robo2* and *robo3* have partially redundant functions in the embryonic central nervous system (Rajagopalan et al., 2000a; Rajagopalan et al., 2000b; Simpson et al., 2000a; Simpson et al., 2000b), we wanted to examine the effect of simultaneous disruption of multiple Robo family proteins in the visual system. However, analysis of Robo family function using existing alleles proved insufficient. First, marked clones of *robo*^{5} mutant tissue were generated in a homozygous *robo3*^{1} background, but no defects were observed (T.D.T. and P.A.G., unpublished). Second, *robo,robo2* double mutant mosaic analysis could not be performed because the necessary animals did not survive to form adult visual systems, and the proximity of the *robo2* and *robo3* genes [87 kb (Simpson et al., 2000b)] prevented the creation of a *robo2,robo3* recombinant. Third, we determined that the only existing mutant allele of *robo3* (*robo3*^{1}), characterized as a strong loss-of-function or null allele in the embryo (Rajagopalan et al., 2000b), produced substantial quantities of full-length Robo3 protein and increased levels of a lower molecular weight form of Robo3 in the adult head (Fig. 4A). Significant amounts of Robo3 immunostaining were also observed in the developing visual system of *robo3*^{1} animals (T.D.T. and P.A.G., unpublished), suggesting that *robo3*^{1} is not a null in the visual system. Therefore, a different strategy was used to achieve simultaneous inhibition of *robo*, *robo2* and *robo3* in the visual system.

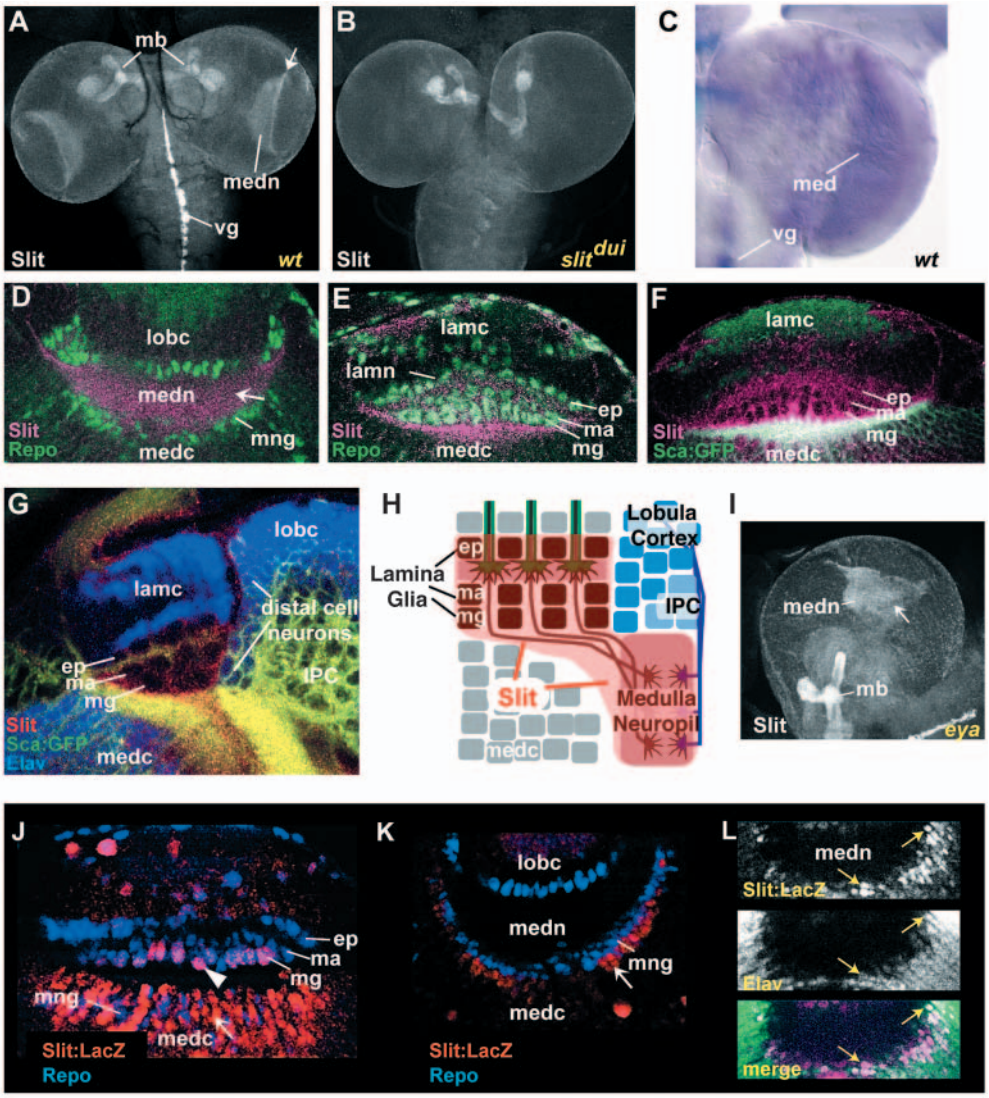

Fig. 4. Slit is expressed in the developing optic lobe. (A,B) Third instar nervous system stained with anti-Slit. (A) Slit is expressed in the medulla neuropil and the base of the lamina (arrow), as well as the ventral ganglion midline and mushroom bodies. (B) In *slit*^{dui} mutants, Slit expression is greatly reduced in the optic lobe and ventral ganglion, although robust mushroom body staining is still observed. (C) Slit mRNA is expressed by cells surrounding the medulla. (D,E) Third instar visual systems stained with anti-Slit (magenta) and anti-Repo (green). (D) Slit protein is found throughout the medulla neuropil (arrow), which is surrounded by medulla neuropil glia. (E) Slit is present in the lamina neuropil and surrounds the epithelial, marginal and medulla glia. (F) Similar view as in E, stained with anti-Slit (magenta) and Sca:GFP (green). (G) Horizontal view stained with anti-Slit (red), anti-Elav (blue) and Sca:GFP (green). Slit protein localizes immediately adjacent to distal cell neurons at the base of the lamina and the optic chiasm. (H) Summary of Slit expression. (I) Third instar *eya*^{2} mutant visual system stained with anti-Slit. Slit protein is expressed in the medulla neuropil (arrow) in the absence of photoreceptor innervation. (I,J) Expression of the *slit*$^{l(2)k05248}$ (Slit:*lacZ*) enhancer trap. (J,K) Optic lobes stained with anti-*lacZ* (red) and anti-Repo (blue). (J) Slit:*lacZ* is expressed in medulla glia (arrowhead) and cells in the medulla cortex (arrow). (K) Slit:*lacZ* cells in medulla cortex (arrow) lie adjacent to medulla neuropil glia. (L) Optic lobe stained with anti-*lacZ* (upper panel), anti-Elav (middle panel) and a merged image (lower panel) with anti-*lacZ* in magenta and anti-Elav in green. Slit:*lacZ* cells in medulla cortex (arrows) coexpress varying levels of neuronal marker Elav. ep, epithelial glia; lamc, lamina cortex; lamn, lamina neuropil; lobc, lobula cortex; ma, marginal glia; mb, mushroom bodies; medc, medulla cortex; medn, medulla neuropil; mg, medulla glia; mng, medulla neuropil glia; vg, ventral ganglion midline.

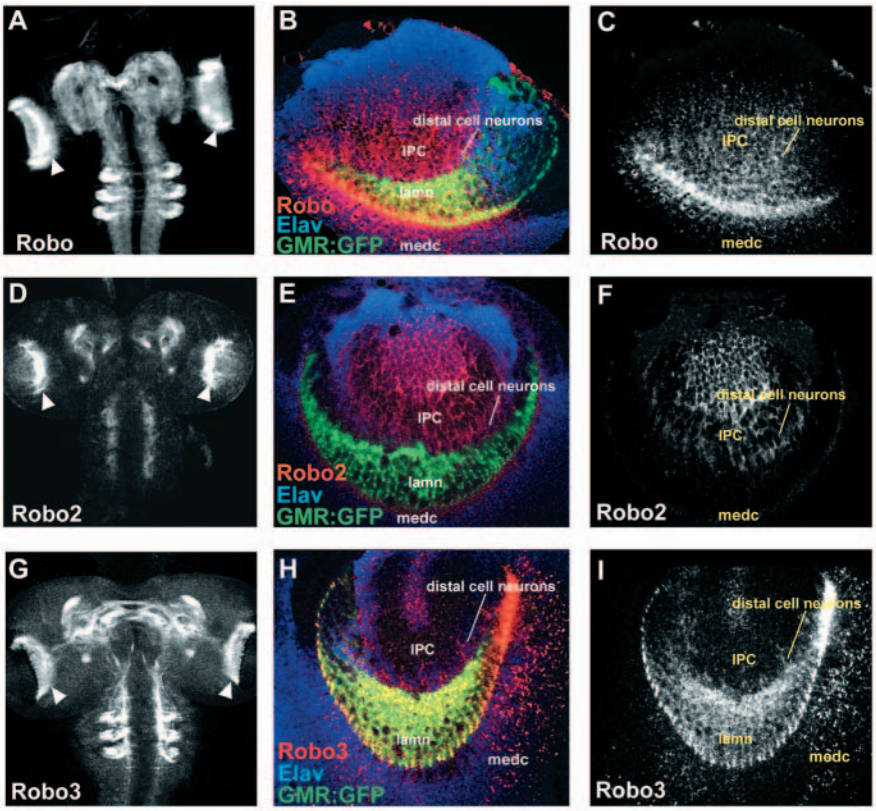

Fig. 5. Robo, Robo2 and Robo3 are expressed in overlapping patterns in the visual system. (A,D,G) Third instar nervous systems stained with antisera against indicated Robo family member. (B,E,H) Lateral view of optic lobe stained with antisera against indicated Robo family member (magenta), neuronal nuclei stained with anti-Elav (blue), and photoreceptor axons visualized with GMR:GFP (green). (C,F,I) Robo family staining alone. (A) Robo is expressed in the developing optic lobes (arrowheads). (B,C) Robo is expressed by IPC neuroblasts, by distal cell neurons, and in the medulla cortex. (D) Robo2 is expressed in the developing optic lobes (arrowheads). (E,F) Robo2 is expressed by IPC neuroblasts and distal cell neurons. (G) Robo3 is expressed in the developing optic lobes (arrowheads). (H,I) Robo3 expression is not detected in IPC neuroblasts, but is detected in distal cell neurons and in the medulla cortex as well as in photoreceptor axons. IPC, inner proliferation center; lamn, lamina neuropil; medc, medulla cortex.

Tissue-specific transgenic RNAi was used to inhibit expression of each of the Robos. *UAS-RoboRNAi*, *UAS-Robo2RNAi* and *UAS-Robo3RNAi* transgenic flies were generated and the transgenes proved effective inhibitors of their targets as assessed using a combination of Western blot analysis and tissue staining (Fig. 6B-M). As shown in Fig. 6E-M, expression of *UAS-RoboRNAi*, *UAS-Robo2RNAi* or *UAS-Robo3RNAi* under the control of Gal4 substantially reduced expression of the corresponding Robo family protein without detectably affecting expression of other Robo family members. Thus, these transgenic RNAi constructs permitted inducible knockdown of each Robo family protein.

Inhibition of Robo family expression causes distal cell neurons to enter the lamina

We examined the function of Robo receptors in the visual system by expressing our UAS-RNAi transgenes under the control of a variety of different Gal4 sources. The nervous system-specific *c155-Gal4* was used to drive expression of transgenic RNAi in optic lobe neuroblasts and neurons. Expression of a single copy of *UAS-RoboRNAi, UAS-Robo2RNAi* or *UAS-Robo3RNAi* under the control of *c155-Gal4* had no effect on visual system development. However, simultaneous inhibition of all three Robos in *c155-Gal4,UAS-GFP,UAS-RoboRNAi,UAS-Robo2RNAi,UAS-Robo3RNAi* animals caused strong visual system phenotypes (Fig. 7A,B). As in *slit* mutants, distal cell neurons invaded the developing lamina in *c155-Gal4, UAS-GFP,UAS-RoboRNAi,UAS-Robo2RNAi,UAS-Robo3RNAi* animals (arrow and arrowhead, Fig. 7B). Thus, Robo family proteins act within the nervous system to prevent distal cell neurons from invading the lamina.

Distal cell neuron defects were also induced by expressing UAS-RNAi transgenes under the control of *Sca-Gal4*, which drives expression in a smaller subset of neuroblasts and neurons than *c155-Gal4*. Expression of a single copy of *UAS-RoboRNAi, UAS-Robo2RNAi* or *UAS-Robo3RNAi*, or simple pairwise combinations of these transgenes under the control of *Sca-Gal4* caused no phenotypes. However, simultaneous inhibition of all three Robos in *Sca-Gal4,UAS-GFP,UAS-RoboRNAi,UAS-Robo2RNAi,UAS-Robo3RNAi* animals caused distal cell neurons to invade the developing lamina (Fig. 7C,D). Simultaneous visualization of lamina glia and distal cell neurons in Robo-knockdown animals further demonstrated the intermingling of distal cell neurons and lamina glia in these animals (Fig. 7E,F, compare with Fig. 1B). These observations indicate that all three Robo family members contribute to preventing distal cells neurons from intermingling with the lamina glia.

As the role of Slit in visual system development was initially identified through its effect on photoreceptor axon targeting, we examined whether photoreceptor axon targeting was similarly dependent upon Robo family receptors. Indeed, generalized inhibition of all three Robo receptors under the control of *Tubulin-Gal4* in *Tubulin-Gal4,UAS-RoboRNAi,UAS-Robo2RNAi,UAS-Robo3RNAi* animals disrupted photoreceptor axon targeting in a fashion similar to that observed in *slit* mutants (Fig. 8A,B). Interestingly, simultaneous expression of *UAS-RoboRNAi,UAS-Robo2RNAi* and *UAS-Robo3RNAi* under the control of the eye-specific Gal4 source *GMR-Gal4* generated no defects in photoreceptor axon targeting (Fig. 8C), while inhibition of Robo family expression using *Sca-Gal4* did disrupt photoreceptor axon targeting (Fig. 8D,E,F). In fact, regions of photoreceptor mistargeting corresponded to regions where *Sca-Gal4* cells (distal cell neurons) entered the lamina (Fig. 8D,E,F). While these knockdown experiments do not preclude a role for Robo family receptors in the photoreceptors, they nonetheless consistent with the misplacement of distal cell neurons contributes to photoreceptor axon mistargeting (Fig. 8G). These data also further emphasize the similarity of the

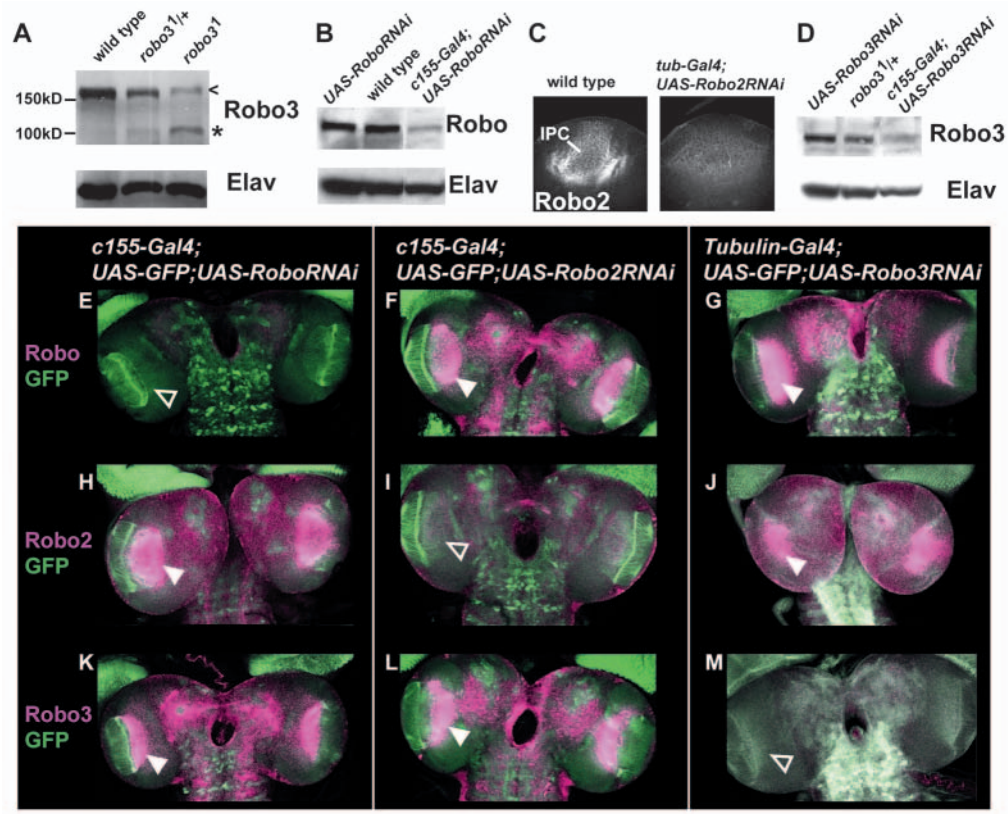

Fig. 6. Knockdown of Robo family proteins using transgenic RNAi. (A) Western blot analysis of adult heads, showing that animals homozygous for *robo3*^{1} express full-length Robo3 protein (caret) as well as a truncated Robo3 (asterisk). Anti-Elav used as loading control. (B) Western blot analysis of adult heads, showing that expression of *UAS:RoboRNAi* in the nervous system controlled by *c155-Gal4* reduces Robo protein levels. (C) Ubiquitous expression of *UAS:Robo2RNAi* under the control of *tubulin-Gal4* reduces anti-Robo2 staining in the visual system. (D) Western blot analysis of adult heads, showing that expression of *UAS-Robo3RNAi* controlled by *c155-Gal4* reduces Robo3 protein levels. (E-M) RNAi of an individual Robo family member does not detectably reduce expression of other Robo family proteins. (E-G) Anti-Robo staining in magenta. (H-J) Anti-Robo2 expression in magenta. (K-M) Anti-Robo3 expression in magenta. (E,H,K) Robo RNAi detectably reduces Robo expression (open arrowhead), but not Robo2 or Robo3 (closed arrowheads). (F,I,L) Robo2 RNAi detectably reduces Robo2 expression (open arrowhead), but not Robo or Robo3 (closed arrowheads). (G,J,M) Robo3 RNAi detectably reduces Robo3 expression (open arrowhead), but not Robo or Robo2 (closed arrowheads).

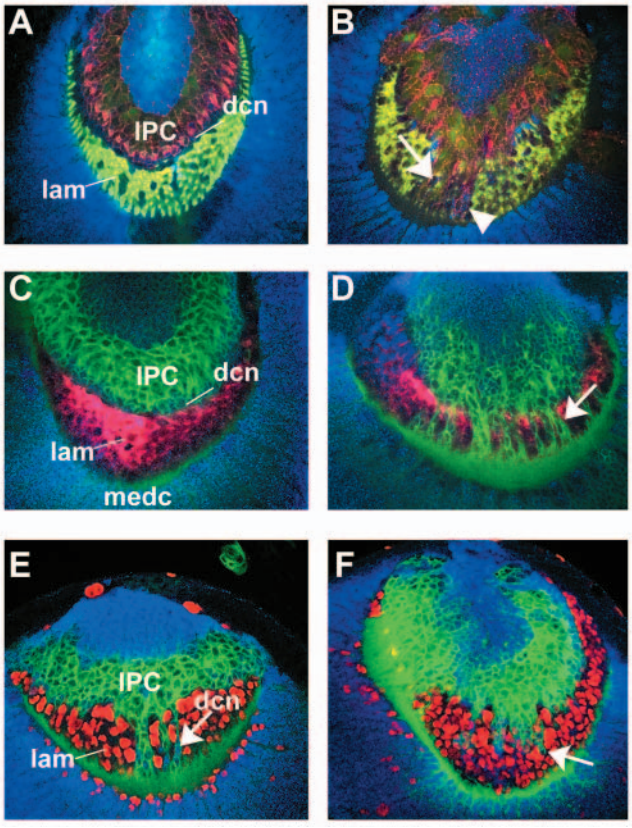

Fig. 7. Distal cell neurons intermingle with lamina glia in Robo family knockdowns. (A,B) Lateral view (anterior at bottom). IPC neuroblasts and distal cell neurons are visualized with anti-Fas3 (red), c155:GFP is most strongly observed in IPC neuroblasts and photoreceptors (green), and neuronal nuclei are visualized with anti-Elav (blue). (A) *c155-Gal4;UAS-GFP*. (B) Distal cell neurons enter the lamina in *c155-Gal4;UAS-GFP;UAS-RoboRNAi;UAS-Robo2RNAi;UAS-Robo3RNAi* animals (arrow), reaching anterior edge of lamina (arrowhead). (C-F) Animals express GFP (green) under control of *Sca-Gal4*, labeling the IPC, distal cell neurons and medulla cortex. Neuronal nuclei are visualized with anti-Elav (blue). (C,D) Photoreceptor axons are visualized using anti-Chaoptin (red). (C) *Sca-Gal4;UAS-GFP* animal. (D) Distal cell neurons enter the lamina in *Sca-Gal4;UAS-GFP;UAS-RoboRNAi;UAS-Robo2RNAi;UAS-Robo3RNAi* animals (arrow). (E,F) Lamina glia are visualized using anti-Repo (red). Distal cell neurons intermingle (arrows) with lamina glia in Robo family knockdown animals. (E) *Sca-Gal4;UAS-GFP;UAS-RoboRNAi,UAS-Robo3RNAi;UAS-RoboRNAi,UAS-Robo3RNAi* animal. (While *Sca-Gal4;UAS-RoboRNAi;UAS-Robo3RNAi* animals had no defects, animals containing two copies of both *UAS-RoboRNAi* and *UAS-Robo3RNAi* had modest defects, consistent with overlapping roles of Robo family members.) (F) *Sca-Gal4;UAS-GFP;UAS-RoboRNAi;UAS-Robo2RNAi;UAS-Robo3RNAi* animal. dcn, distal cell neuron progeny; IPC, inner proliferation center; lam, lamina; medc, medulla cortex.

effects of knockdown of Robo family receptors and reductions in Slit expression on optic lobe morphogenesis.

Discussion

The construction of anatomically distinct processing centers in the brain is a complex morphogenetic task that requires segregation of adjacent groups of cells. Despite the extensive study of how cells are segregated into distinct groups, the identities of the molecules that prevent intermingling between adjacent groups remain largely unknown (Dahmann and Basler, 1999; Irvine and Rauskolb, 2001; McNeill, 2000; Vegh and Basler, 2003). Here we have identified a novel role for Slit and the Robo receptors as key factors that prevent mixing between adjacent groups of cells in the fly brain. We have focused on the effect of Slit and Robo family proteins on the boundary between the glia at the posterior edge of the lamina and the neurons at the anterior edge of the lobula cortex. We have found that the secreted protein Slit surrounds the lamina glia on one side of the boundary while Robo family proteins (receptors for Slit) are expressed by the distal cell neurons on the other side of the boundary. We show that loss of Slit expression or tissue-specific inhibition of Robo family expression in distal cell neurons causes the intermingling of lamina glia and distal cell neurons. We propose that Slit protein in the lamina keeps Robo-expressing neurons within the normal confines of the lobula cortex, establishing the sharp boundary between these two regions. Given the conservation of Slit and Robo signaling in axon guidance throughout evolution, Slit and Robo family members may also regulate boundary formation in the brains of other animals. Interestingly, humans with mutations in *ROBO3* exhibit defects in hindbrain morphology, although the underlying developmental defect in humans is not known (Jen et al., 2004).

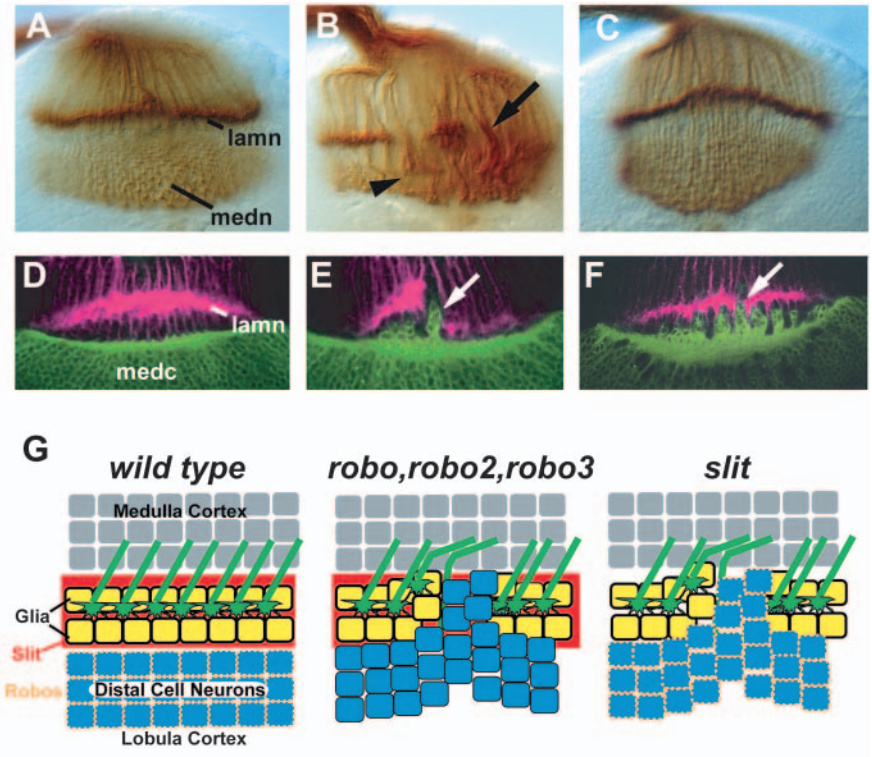

Fig. 8. Robo family knockdown disrupts photoreceptor axon targeting. (A-C) Photoreceptor axons visualized using anti-Chaoptin. (A) *Tubulin-Gal4;UAS-GFP* control. (B) *Tubulin-Gal4;UAS-GFP;UAS-RoboRNAi;UAS-Robo2RNAi;UAS-Robo3RNAi* animal, showing many photoreceptor axons extending through the lamina (arrow) and too many photoreceptor axons entering the medulla (arrowhead). (C) *GMR-Gal4;UAS-GFP;UAS-RoboRNAi;UAS-Robo2RNAi;UAS-Robo3RNAi* animal. (D-F) Animals express GFP (green) under control of *Sca-Gal4*, while photoreceptor axons are visualized using anti-Chaoptin (magenta). (D) *Sca-Gal4;UAS-GFP* animal. (E) *Sca-Gal4;UAS-GFP;UAS-RoboRNAi,UAS-Robo3RNAi;UAS-RoboRNAi,UAS-Robo3RNAi* animal in which GFP-expressing cells in the lamina correspond to regions of photoreceptor axon mistargeting (arrow). (F) *Sca-Gal4;UAS-GFP;UAS-RoboRNAi;UAS-Robo2RNAi;UAS-Robo3RNAi* animal. (G) Schematic of observed disruptions in visual system development. In wild type, distal cell neurons (blue) express Robos (orange outline), while Slit protein (red) surrounds glia (yellow with black outline) at the base of the lamina. Lamina glia serve as initial targets of incoming R1-R6 photoreceptor axons (green). When expression of all three Robo family members is inhibited in distal cell neurons (*robo*, *robo2*, *robo3*), distal cell neurons intermingle with the lamina glia and photoreceptor axon targeting is disrupted. Loss of Slit expression (*slit*) causes an indistinguishable defect.

Slit and Robo family proteins are regulators of boundary maintenance

Compartmentalization is important throughout nervous system development (Pasini and Wilkinson, 2002), and structural compartmentalization underlies functional compartmentalization in the adult brain. The adult vertebrate brain contains many distinct compartments, such as Brodmann's areas of the cerebral cortex and the brainstem nuclei, and anatomical studies point to similar compartmentalization in the *Drosophila* brain (Younossi-Hartenstein et al., 2003). As noted above, several molecules that regulate cell adhesion or cell repulsion have been implicated in restricting cell mixing between compartments in the developing nervous system, but loss of these proteins has not been shown to cause intermingling between compartments. Here we have shown that Slit and the Robos are required to prevent cell intermingling across a boundary in the optic lobe.

We determined that knockdown of Robo family protein expression in the optic lobe using the *Sca-Gal4* driver caused robust defects in distal cell neuron positioning. In addition to driving gene expression in the inner proliferation center neuroblasts and distal cell neurons, *Sca-Gal4* also drives expression in R8 photoreceptor axons and neuroblasts of the outer proliferation center and neurons of the medulla cortex. As noted above, inhibition of Robo family expression only in the photoreceptors caused no detectable defects. In addition, knockdown of all three Robo family proteins in the medulla cortex using *apterous-Gal4* had no effect on distal cell neuron behavior, and no defects in medulla neuron movement or axon targeting were identified in either *slit* mutants or Robo family knockdowns (T.D.T. and P.A.G., unpublished). Taken together

with Robo family protein expression data, the Robo family knockdown analysis strongly supports a requirement for Robo family receptors in distal cell neurons in preventing them from invading the lamina neuropil.

Slit and Robo family protein expression in the optic lobe

In the *Drosophila* visual system, Slit protein is present in a continuous zone from the base of the lamina into the underlying medulla neuropil. Although Slit mRNA is detected within the optic lobe, and Slit:*lacZ* expression is detected in medulla glia at the base of the lamina and in medulla cortex neurons, the optic lobe does not appear highly sensitive to the precise source or concentration of Slit. Attempts to use mosaic analysis to further define the cells in which *slit* function was required were unsuccessful, as no phenotypes were observed, despite the generation of large marked patches of $slit^2$ mutant tissue in the visual system and the use of the Minute technique to maximize mutant clone size (T.D.T. and P.A.G., unpublished). We suspect that the diffusibility of Slit protein combined with the large number of Slit-expressing cells in the optic lobe permitted the remaining heterozygous and wild-type cells in the mosaic animals to provide sufficient Slit to support proper optic lobe development. In addition, expression of Slit in photoreceptors under the control of *GMR-Gal4* rescued the photoreceptor projection phenotype of *slit* mutants as effectively as more general expression of Slit in the optic lobe using *Omb-Gal4*. Thus, delivery of Slit to these neuropil regions may be sufficient to restore the boundary between the lobula cortex and the lamina.

We also examined the effects of overexpression and ectopic expression of Slit and Robo proteins in the optic lobe. Overexpression of Slit in the optic lobe using *GMR*-Gal4, *Sca-Gal4, Omb-Gal4* or the more ubiquitously expressed *Tubulin-Gal4* did not generate detectable phenotypes in the optic lobe (T.D.T. and P.A.G., unpublished). The failure to generate strong overexpression phenotypes could reflect the increased Slit expression within the lamina that accompanied overexpression in other regions using these Gal4 drivers. However, overexpression of Robo2 under the control of *Sca-Gal4* dramatically distorted the shape of the lobula cortex, causing the distal cell neurons to move around the ventral and dorsal edges of the lamina (T.D.T. and P.A.G., unpublished). As distal cell neurons normally encounter Slit protein at the posterior face of the lamina, this redistribution could reflect repulsion from regions of Slit expression. Overexpression of Robo or Robo3 caused no detectable defects.

Robo family proteins appear to localize around the cell body periphery of newly differentiated distal cell neurons. This cell-body-associated expression contrasts with the predominantly axonal expression of Robo family proteins by more mature lobula cortex neurons. Whether this reflects a regulated shift in the subcellular localization of Robo proteins, or simply the availability of axonal processes in more mature neurons, is unknown. However, as Slit and Robo family proteins control both neuronal migration and axon navigation (Wong et al., 2002), such a change in Robo family protein distribution could alter the response of a neuron to Slit from one involving the cell body to one preferentially involving the axon. We have not detected obvious misprojections of the axons of the distal cell neurons in our mutants (T.D.T. and P.A.G., unpublished), although subtle defects in targeting of these axons would not be detected using available markers.

Regulation of cell mixing at boundaries in the developing brain

Boundaries are commonly encountered during development, and several mechanisms have been proposed for preventing mixing between compartments. Our observations provide evidence for a signal associated with one cell population preventing the invasion of a neighboring cell population expressing receptors for that signal. Interestingly, even when the distal cell neurons invade the lamina in *slit* mutants or Robo family knockdown animals, they do not disperse evenly among the lamina glia. Rather, the distal cell neurons remain preferentially associated with one another, suggesting the persistence of differential adhesion when the Slit signal is absent. Thus, multiple parallel mechanisms, possibly involving both repulsion and differential adhesion, are potentially involved in maintaining the normally precise distinction between lamina and lobula cortex. Combinations of adhesion and repulsion may act at other boundaries, providing robustness as well as functional redundancy to the molecular mechanisms of compartment maintenance.

We thank C. Goodman, J. Simpson, R. Jacobs, B. Dickson and G. Bashaw for generously providing many antibodies and fly stocks. We thank I. Rebay and Garrity lab members for helpful discussions, and L. Huang and J. Whited for comments on the manuscript. This work was supported by grants to P.A.G. from the National Eye Institute, the Raymond and Beverly Sackler Foundation, and the McKnight Foundation. T.D.T. was supported by an NIH Predoctoral Training Grant.

References

Battye, R., Stevens, A., Perry, R. L. and Jacobs, J. R. (2001). Repellent signaling by Slit requires the leucine-rich repeats. *J. Neurosci.* **21**, 4290-4298.

Brand, A. H. and Perrimon, N. (1993). Targeted gene expression as a means of altering cell fates and generating dominant phenotypes. *Development* **118**, 401-415.

Brose, K. and Tessier-Lavigne, M. (2000). Slit proteins: key regulators of axon guidance, axonal branching, and cell migration. *Curr. Opin. Neurobiol.* **10**, 95-102.

Brose, K., Bland, K. S., Wang, K. H., Arnott, D., Henzel, W., Goodman, C. S., Tessier-Lavigne, M. and Kidd, T. (1999). Slit proteins bind Robo receptors and have an evolutionarily conserved role in repulsive axon guidance. *Cell* **96**, 795-806.

Campbell, G., Goring, H., Lin, T., Spana, E., Andersson, S., Doe, C. Q. and Tomlinson, A. (1994). RK2, a glial-specific homeodomain protein required for embryonic nerve cord condensation and viability in Drosophila. *Development* **120**, 2957-2966.

Cheng, Y. C., Amoyel, M., Qiu, X., Jiang, Y. J., Xu, Q. and Wilkinson, D. G. (2004). Notch activation regulates the segregation and differentiation of rhombomere boundary cells in the zebrafish hindbrain. *Dev. Cell* **6**, 539-550.

Cooke, J. E. and Moens, C. B. (2002). Boundary formation in the hindbrain: Eph only it were simple. *Trends Neurosci.* **25**, 260-267.

Cordes, S. P. and Barsh, G. S. (1994). The mouse segmentation gene kr encodes a novel basic domain-leucine zipper transcription factor. *Cell* **79**, 1025-1034.

Dahmann, C. and Basler, K. (1999). Compartment boundaries: at the edge of development. *Trends Genet.* **15**, 320-326.

Dearborn, R., Jr and Kunes, S. (2004). An axon scaffold induced by retinal axons directs glia to destinations in the Drosophila optic lobe. *Development* **131**, 2291-2303.

Dumstrei, K., Wang, F., Nassif, C. and Hartenstein, V. (2003). Early

development of the Drosophila brain: V. Pattern of postembryonic neuronal lineages expressing DE-cadherin. *J. Comp. Neurol.* **455**, 451-462.

Englund, C., Steneberg, P., Falileeva, L., Xylourgidis, N. and Samakovlis, C. (2002). Attractive and repulsive functions of Slit are mediated by different receptors in the Drosophila trachea. *Development* **129**, 4941-4951.

Garrity, P. A., Rao, Y., Salecker, I., McGlade, J., Pawson, T. and Zipursky, S. L. (1996). Drosophila photoreceptor axon guidance and targeting requires the Dreadlocks SH2/SH3 adapter protein. *Cell* **85**, 639-650.

Hartenstein, V., Nassif, C. and Lekven, A. (1998). Embryonic development of the Drosophila brain. II. Pattern of glial cells. *J. Comp. Neurol.* **402**, 32-47.

Hofbauer, A. and Campos-Ortega, J. A. (1990). Proliferation pattern and early differentiation of the optic lobes in Drosophila melanogaster. *Roux's Arch. Dev. Biol.* **198**, 264-274.

Inoue, T., Tanaka, T., Takeichi, M., Chisaka, O., Nakamura, S. and Osumi, N. (2001). Role of cadherins in maintaining the compartment boundary between the cortex and striatum during development. *Development* **128**, 561-569.

Irvine, K. D. and Rauskolb, C. (2001). Boundaries in development: formation and function. *Annu. Rev. Cell Dev. Biol.* **17**, 189-214.

Jen, J. C., Chan, W. M., Bosley, T. M., Wan, J., Carr, J. R., Rub, U., Shattuck, D., Salamon, G., Kudo, L. C., Ou, J. et al. (2004). Mutations in a human ROBO gene disrupt hindbrain axon pathway crossing and morphogenesis. *Science* **304**, 1509-1513.

Kalidas, S. and Smith, D. P. (2002). Novel genomic cDNA hybrids produce effective RNA interference in adult Drosophila. *Neuron* **33**, 177-184.

Karpen, G. H. and Spradling, A. C. (1992). Analysis of subtelomeric heterochromatin in the Drosophila minichromosome. *Genetics* **132**, 737-753.

Kidd, T., Bland, K. S. and Goodman, C. S. (1999). Slit is the midline repellent for the robo receptor in Drosophila. *Cell* **96**, 785-794.

Kramer, S. G., Kidd, T., Simpson, J. H. and Goodman, C. S. (2001). Switching repulsion to attraction: changing responses to slit during transition in mesoderm migration. *Science* **292**, 737-740.

Larsen, C. W., Zeltser, L. M. and Lumsden, A. (2001). Boundary formation and compartition in the avian diencephalon. *J. Neurosci.* **21**, 4699-4711.

Lee, T. and Luo, L. (1999). Mosaic analysis with a repressible cell marker for studies of gene function in neuronal morphogenesis. *Neuron* **22**, 451-461.

Lumsden, A. and Krumlauf, R. (1996). Patterning the vertebrate neuraxis. *Science* **274**, 1109-1115.

McNeill, H. (2000). Sticking together and sorting things out: adhesion as a force in development. *Nat. Rev. Genet.* **1**, 100-108.

Meinertzhagen, I. A. and Hanson, T. E. (1993). The development of the optic lobe. In *The development of Drosophila melanogaster* (ed. M. Bate and A. Martinez-Arias), pp. 1363-1491. Cold Spring Harbor, NY: Cold Spring Harbor Laboratory Press.

Meinertzhagen, I. A., Emsley, J. G. and Sun, X. J. (1998). Developmental anatomy of the Drosophila brain: neuroanatomy is gene expression. *J. Comp. Neurol.* **402**, 1-9.

Mellitzer, G., Xu, Q. and Wilkinson, D. G. (1999). Eph receptors and ephrins restrict cell intermingling and communication. *Nature* **400**, 77-81.

Milan, M., Weihe, U., Perez, L. and Cohen, S. M. (2001). The LRR proteins capricious and Tartan mediate cell interactions during DV boundary formation in the Drosophila wing. *Cell* **106**, 785-794.

Nassif, C., Noveen, A. and Hartenstein, V. (2003). Early development of the Drosophila brain: III. The pattern of neuropile founder tracts during the larval period. *J. Comp. Neurol.* **455**, 417-434.

Nose, A., Nagafuchi, A. and Takeichi, M. (1988). Expressed recombinant cadherins mediate cell sorting in model systems. *Cell* **54**, 993-1001.

Pasini, A. and Wilkinson, D. G. (2002). Stabilizing the regionalisation of the developing vertebrate central nervous system. *BioEssays* **24**, 427-438.

Rajagopalan, S., Nicolas, E., Vivancos, V., Berger, J. and Dickson, B. J. (2000a). Crossing the midline: roles and regulation of Robo receptors. *Neuron* **28**, 767-777.

Rajagopalan, S., Vivancos, V., Nicolas, E. and Dickson, B. J. (2000b). Selecting a longitudinal pathway: Robo receptors specify the lateral position of axons in the Drosophila CNS. *Cell* **103**, 1033-1045.

Rangarajan, R., Gong, Q. and Gaul, U. (1999). Migration and function of glia in the developing Drosophila eye. *Development* **126**, 3285-3292.

Redies, C. (2000). Cadherins in the central nervous system. *Prog. Neurobiol.* **61**, 611-648.

Redies, C. and Puelles, L. (2001). Modularity in vertebrate brain development and evolution. *BioEssays* **23**, 1100-1111.

Schneider-Maunoury, S., Seitanidou, T., Charnay, P. and Lumsden, A. (1997). Segmental and neuronal architecture of the hindbrain of Krox-20 mouse mutants. *Development* **124**, 1215-1226.

Simpson, J. H., Bland, K. S., Fetter, R. D. and Goodman, C. S. (2000a). Short-range and long-range guidance by Slit and it Robo receptors: a combinatorial code of Robo receptors controls lateral position. *Cell* **103**, 1019-1032.

Simpson, J. H., Kidd, T., Bland, K. S. and Goodman, C. S. (2000b). Short-range and long-range guidance by Slit and its Robo receptors: Robo and Robo2 play distinct roles in midline guidance. *Neuron* **28**, 753-766.

Torok, T., Tick, G., Alvarado, M. and Kiss, I. (1993). P-lacW insertional mutagenesis on the second chromosome of Drosophila melanogaster: isolation of lethals with different overgrowth phenotypes. *Genetics* **135**, 71-80.

Vegh, M. and Basler, K. (2003). A genetic screen for hedgehog targets involved in the maintenance of the Drosophila anteroposterior compartment boundary. *Genetics* **163**, 1427-1438.

Wolff, T. (2000). Histological Techniques for the Drosophila Eye. Part II: Adult. In *Drosophila Protocols* (ed. W. Sullivan, M. Ashburner and R. S. Hawley), pp. 224-243. Cold Spring Harbor, NY: Cold Spring Harbor Laboratory Press.

Wong, K., Park, H. T., Wu, J. Y. and Rao, Y. (2002). Slit proteins: molecular guidance cues for cells ranging from neurons to leukocytes. *Curr. Opin. Genet. Dev.* **12**, 583-591.

Xu, Q., Mellitzer, G., Robinson, V. and Wilkinson, D. G. (1999). In vivo cell sorting in complementary segmental domains mediated by Eph receptors and ephrins. *Nature* **399**, 267-271.

Xu, Q., Mellitzer, G. and Wilkinson, D. G. (2000). Roles of Eph receptors and ephrins in segmental patterning. *Philos. Trans. R. Soc. Lond., B, Biol. Sci.* **355**, 993-1002.

Younossi-Hartenstein, A., Nassif, C., Green, P. and Hartenstein, V. (1996). Early neurogenesis of the Drosophila brain. *J. Comp. Neurol.* **370**, 313-329.

Younossi-Hartenstein, A., Salvaterra, P. M. and Hartenstein, V. (2003). Early development of the Drosophila brain: IV. Larval neuropile compartments defined by glial septa. *J. Comp. Neurol.* **455**, 435-450.

Zeltser, L. M., Larsen, C. W. and Lumsden, A. (2001). A new developmental compartment in the forebrain regulated by Lunatic fringe. *Nat. Neurosci.* **4**, 683-684.